# Optimised Process to Produce Calcium Acetate from Waste Blue Mussel Shells and its Use as a De-icer

**Jennifer N. Murphy, Melissa A. Morgan, Sachel Christian-Robinson, Megan M. Fitzgerald and Francesca M. Kerton***

Department of Chemistry, Memorial University of Newfoundland, St. John's, NL, A1B 3X7, Canada. * Corresponding author e-mail: fkerton@mun.ca; Tel: +1-709-864-8089

† *Dedicated to Steve Westcott in memory of his inspiring friendship and the warm welcome to Atlantic Canada. Thank you for the many beers and listening ear, and from our cats – thank you for the treats and toys.*

## Abstract

The preparation of calcium acetate from mussel (*Mytilus edulis*) shells and acetic acid was optimised via design of experiments. The solid product was identified as the monohydrate via powder X-ray diffraction, IR spectroscopy and Thermogravimetric analysis. Comparisons were made to optical grade calcite in place of the bio-sourced calcium carbonate for the synthesis. An exploratory central composite design compared the yield of calcium acetate with respect to shell material used (shells dried in air at room temperature, dried at 220 °C or calcined), concentration of acetic acid, and time. The yield of $Ca(CH_3COO)_2 \cdot H_2O$ was optimized further using heated, crushed shells using a custom optimal design. A maximum yield of 93% was reached after 32 h using 9% v/v $CH_3COOH$ or an 85% yield using food-grade white vinegar after 24 h. De-icing

experiments showed that $Ca(CH_3COO)_2 \cdot H_2O$ produced from waste blue mussel shells melted 6 wt.% of ice at a concentration of 30% (m/v). For comparison, 11 wt.% defrosted using $CaCl_2$ 30% (m/v) and 13 wt.% defrosted using NaCl 30% (m/v).

## Introduction

Mussel shells are a valuable source of $CaCO_3$ (> 95%) and as such have been valorized in many applications where $CaCO_3$ is used.[1-3] One area where mollusc shells have been underutilized is as a starting material for synthesis. This may be due to purity issues, as molluscs contain organic matter including silk fibroin-like proteins, acidic glycoproteins and β-chitin. Furthermore, studies have shown that there are also small amounts of other minerals present that leads to the presence of the following metals Pb, Hg, Cr, Mg and Fe.[4, 5] Barro *et al.* developed a plant in Spain to make high purity $CaCO_3$ (> 95%) by calcining mussel shells up to 600 °C.[6] The resulting $CaCO_3$ contained $MgCO_3$ and organic carbon as the largest contaminants.

Calcium acetate ($Ca(CH_3COO)_2$) can be made by reacting $CaCO_3$ or CaO with acetic acid ($CH_3COOH$). $Ca(CH_3COO)_2$ can be used medicinally to treat high levels of phosphate in dialysis patients.[7] $Ca(CH_3COO)_2$ can also be used in the preparation of hydroxyapatite,[8] which is used for biomedical applications such as bone and coatings of metal implants, and is an approved food additive in Canada, as an acidity regulator.[9] $Ca(CH_3COO)_2$ can be used as an environmentally friendly de-icer in place of NaCl, however, it is currently not a commercial de-icer. A de-icer is a chemical, mainly salts, that are effective at removing ice or snow and preventing the formation of ice by reducing the freezing point of water.[10] In Canada and much of North America, the use of de-icing agents is critical to keep roadways safe and open during the winter months. The use of road salts minimizes traffic accidents, injuries and deaths during ice and snow conditions.[11] Road

salt (mainly NaCl) has been used as a de-icing agent in Canada since the 1940s.[12] On average, 5 million tonnes of road salt are used each winter to keep roadways across the country safe. There are several concerns with the use of road salt regarding the environment, infrastructure, and human health. The use of road salts is linked to the salinization of fresh water and corrosion.[13] NaCl is corrosive and non-degradable. Layers of differing densities can exist in lakes due to high salt concentrations and it causes depletion of oxygen in deeper regions of lakes due to incomplete seasonal mixing. This improper mixing leads to the inability of the lake to distribute valuable nutrients to the lake as well and may lead to ecosystem changes. Prolonged chloride concentrations in excess of 250 mg/L is detrimental to aquatic life.[14] Increases in sodium concentrations accelerates the growth of blue-green algae which makes freshwater sources prone to algal blooms. Acetate-based de-icers, such as biodegradable and non-corrosive calcium magnesium acetate ($CaMg_2(CH_3COO)_6$), can also affect the environment. The biodegradation of the acetate ion causes a depletion of oxygen which can cause plant death. The harmful effects of any type of road salt are mainly observed in slow moving waterways where dilution is slow.[15] Acetate based de-icers also affect the integrity of concrete[16] but not to the same degree as chloride based de-icers.[10]

$CaMg_2(CH_3COO)_6$ is 30 times more expensive than rock salt (NaCl) and made from the reaction of dolomite ($CaCO_3$ with at least 5% $MgCO_3$) with $CH_3COOH$.[17] As a result, $CaMg_2(CH_3COO)_6$ is less commonly used on highways and its use is limited to environmentally sensitive regions including bridges.[18] However, the use of renewable feedstocks, such as by-products from the food industry, can make acetate-based de-icers cheaper. De-icers have been made from renewable sources of organic and inorganic materials. $CaMg_2(CH_3COO)_6$ and calcium magnesium propionate have been prepared via fermentation,[18] $Ca(CH_3COO)_2$ has been made using bamboo vinegar,[19] and a variety of de-icers have been made using degradation products from corn steep

water.[20] These show organic materials can be sourced from fermentation of biomass and does not need to be sourced from oil resources. $Ca(CH_3COO)_2$ has previously been prepared using mollusc shells.[21-24] $Ca(CH_3COO)_2$ has been prepared using waste oyster shells and food-grade applications were targetted,[23, 24] and other researchers have targeted de-icing applications using waste oysters or clam shell powder.[21, 22] There was a language barrier in understanding some of the literature.[22, 24] Herein, we describe the synthesis of $Ca(CH_3COO)_2$ from waste blue mussel (BM) shells and the use of this material as a de-icing agent. $Ca(CH_3COO)_2$ is currently not on the market as an anti-ice or de-icing agent. Few studies have been performed on calcium acetate as a de-icer,[19] but it has been reported that $Ca(CH_3COO)_2$ has a lower freezing point than NaCl (based on same molarity solutions), is an effective de-icer and is less corrosive than NaCl.[19] The use of mussel shells in the preparation of a bio-degradable road salt has the potential to change the outlook on NaCl use in rural communities where mussel processing occurs. Design of experiments (DoE) methodology was used herein to investigate three factors believed to be most influential to a green synthesis of calcium acetate using waste BM shells and to optimize the yield of $Ca(CH_3COO)_2$. The $Ca(CH_3COO)_2$ products were characterized and experiments to test its de-icing capability are presented alongside results for more typical de-icers, namely NaCl (rock salt) and $CaCl_2$.

## Results and Discussion

Typically, when molluscs have been employed as catalysts, adsorbents, or amendments, they have been ground into a fine powder.[3] The reaction of ground mussel shells with acetic acid was evaluated for the synthesis of $Ca(CH_3COO)_2$. Unfortunately, shells ground in a stainless-steel mixer mill had visible iron contamination. For example, the resultant mixture of mussel shells and acetic acid was black, and even after filtering the $Ca(CH_3COO)_2$ solution was strongly coloured,

and iron filings were found on the stir bar after the reaction. Contamination from milling equipment is related to the materials the mill is made out of and its hardness.[25] Unfortunately, we did not have access to mixer vessels made of a harder material. An agate vessel was used to avoid the contamination but as it is a relatively soft material this led to the vessel being damaged. Therefore, the synthesis of $Ca(CH_3COO)_2$ was performed using manually crushed shells.

**Exploratory Experimental Design for the Synthesis of Calcium Acetate**

Design of Experiments allows scientists to construct relationships between a range of variables using data from a series of experiments – it can help avoid assumptions during optimization that can occur when studying only one factor at a time. Initially, a central composite circumscribed (CCC) design was used to investigate the effect of time, concentration of $CH_3COOH$ ([$CH_3COOH$]), and shell pretreatment method (Shell Type) on the yield of calcium acetate with the goal of maximizing the yield, Table 1, shows the factors studied and their respective levels.

**Table 1** Exploratory central composite circumscribed design factors and levels for the synthesis of calcium acetate from mussel shell materials. Three shell types were studied; untreated shells (RTC, room temperature crushed), shells heated at 220 °C for 48 h (HTC, high temperature crushed), and calcined shells (CC, calcined crushed). Shells were crushed into small pieces of less than 2 cm in diameter.

| Name | Factor | -α | -1 | 0 | +1 | +α |
|---|---|---|---|---|---|---|
| A | % $CH_3COOH$ | 2.9 | 5 | 10 | 15 | 17.1 |
| B | Time (h) | 2.3 | 6 | 15 | 24 | 27.7 |
| C | Shell Type | - | RTC | HTC | CC | - |

To study the effect of time, the gap between the levels was made large so any effect could be seen more clearly. The low level (-1) was 6 h and 24 h was used for the high level (+1). The

axial points were 2.3 h (-α) and 27.7 h (+α), respectively. These levels were chosen because they were convenient for timing purposes. The high and low levels for [$CH_3COOH$] were chosen after reading related literature and patents, and based on the requirement for sufficient solution volumes to cover the shells in the flask. For [$CH_3COOH$], the low level (-1) was 5% $CH_3COOH$ and the high level (+1) was 15% $CH_3COOH$. The axial points were 2.9% $CH_3COOH$ (-α) and 17.1% $CH_3COOH$ (+α), respectively. The molar concentrations of these solutions correspond to 0.53, 0.88, 1.8, 2.6 and 3.0 mol/L, respectively. Molar [$CH_3COOH$] observed in literature range from 0.5–10 mol/L.[6, 21, 24] The effect of shell type was a categorical factor, unlike time and [$CH_3COOH$] which are numerical and can be changed easily. It was assumed that the HTC shells would afford higher yields because of its higher purity (less organic matrix present in the shell) but RTC shells were explored as well because of potential environmental benefits (i.e. lower energy considerations). The calcined shells were used to compare the reactivity of a CaO starting material (CC) with the two $CaCO_3$ starting materials (RTC and HTC). Volumes of $CH_3COOH$ were calculated based on the moles required to react with masses of shells assuming shells to be 100% $CaCO_3$ (or CaO in the case of CC). The yields for the many experiments of this design are found in Supplementary Material (Table S1). Analysis of variance revealed all factors were significant in this exploratory design. There was an interaction between shell type and [$CH_3COOH$] and the square of [$CH_3COOH$] was significant as well, giving the model a quadratic shape. The analysis of variance and plots of the residuals are also provided in Supplementary Material. Since this model was only used for exploratory experiments the model was not used for prediction, but it was used to develop another experimental design to further optimize the yield using RTC and HTC shells.

For the exploratory experiments, the empirical models for the response (yield) in terms of the factors studied (time, % $CH_3COOH$, and shell type) are plotted in three-dimensional diagrams (Figures 1-3). Figure 1 shows the model for the yield of $Ca(CH_3COO)_2$ based on time and [$CH_3COOH$] using CC shells. This shows that the yields of $Ca(CH_3COO)_2$ are quite poor, around 50-60%, and do not change much with respect to time and [$CH_3COOH$] variance. These results were surprising because CaO dissolves readily in water producing $Ca(OH)_2$ which is a stronger base than $CaCO_3$. No powder XRD was performed on CC shells so some $CaCO_3$ may still have been present. The yield of $Ca(CH_3COO)_2$ increased as time increased but [$CH_3COOH$] did not affect the yield. The maximum yield achieved with CC shells was 61% after 15 h using 10% $CH_3COOH$. As the non-calcined shells (HTC and RTC) gave higher yields of $Ca(CH_3COO)_2$, the CC shells were note studied further.

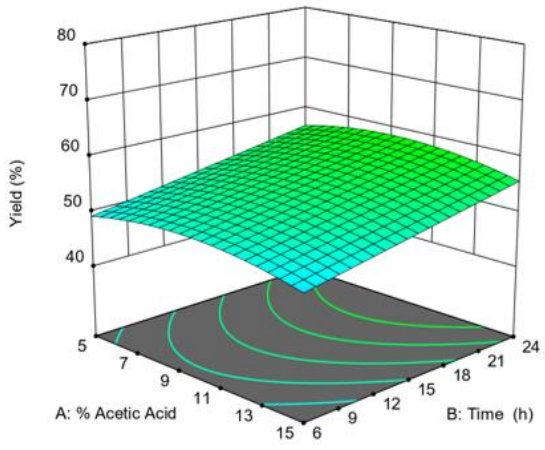


**Figure 1** The response surface plot of yield of $Ca(CH_3COO)_2$ based on concentration of acetic acid and time using calcined mussel shells (CC).

Figure 2 shows the model of $Ca(CH_3COO)_2$ yield based on time and [$CH_3COOH$] using RTC shells from the preliminary CCC studies. This figure shows that the yield of $Ca(CH_3COO)_2$ increases as time increases and as [$CH_3COOH$] decreases. Additionally, the $Ca(CH_3COO)_2$ yields

achieved are higher than using CC shells. This was promising because RTC have not undergone any heat treatment and it would be more economical and sustainable to use these shells for the synthesis. The maximum yield achieved with RTC shells was 66% after 15 h using 2.9% $CH_3COOH$.

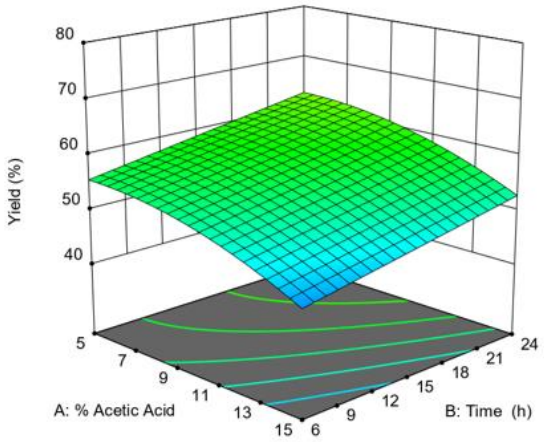


**Figure 2** The response surface plot of yield of calcium acetate (CA) based on concentration of acetic acid and time using raw mussel shells (RTC).

Figure 3 shows the model of $Ca(CH_3COO)_2$ yield based on time and $[CH_3COOH]$ using HTC shells. It shows that the yield of $Ca(CH_3COO)_2$ has the same trend as for RTC shells; the yield of $Ca(CH_3COO)_2$ increases as time increases and as $[CH_3COOH]$ decreases. The modelled yield of $Ca(CH_3COO)_2$ is the highest for HTC shells if all three shell-types and models are compared. This is not surprising as it is known that heat treatment degrades the organic matrix within the shells. The degradation increases the purity of the $CaCO_3$ and increases the surface area of the shells. The maximum yield achieved in these exploratory experiments with HTC shells was 77% after 15 h using 2.9% $CH_3COOH$.

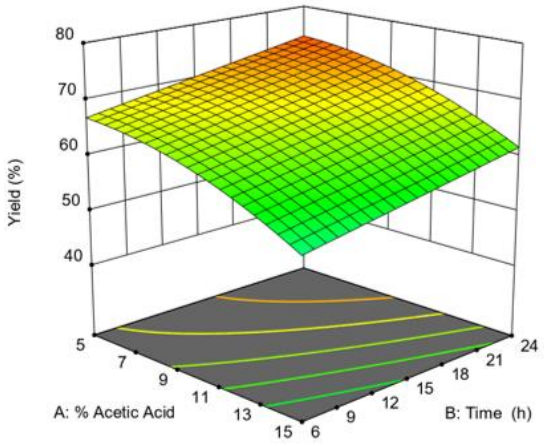


**Figure 3** The response surface plot of yield of $Ca(CH_3COO)_2$ based on concentration of acetic acid and time using heated mussel shells (HTC).

The results of the initial exploratory experiments for the synthesis of $Ca(CH_3COO)_2$ from waste mussel shells provided several insights important for further development towards an optimized yield of $Ca(CH_3COO)_2$. (1) Calcined shells (CC) produced the lowest yields of $Ca(CH_3COO)_2$, (2) RTC and HTC shells had the same trends with respect to time and $[CH_3COOH]$; yield of $Ca(CH_3COO)_2$ increased with increasing time and decreasing $[CH_3COOH]$ and (3) HTC shells gave the best yields of $Ca(CH_3COO)_2$, potentially due to an increased surface area and purity. Because of the poor performance of CC shells and the lack of sustainability associated with calcining shells, the yield of $Ca(CH_3COO)_2$ was not optimized further using CC as a source of CaO. RTC shells were not used going forward because of the distinct advantage of the higher purity and surface area of HTC shells. Therefore, a new experimental design was developed focused on HTC shells only. To maximize the yield of $Ca(CH_3COO)_2$, the path of steepest ascent in the model of yield must be followed. Therefore, the time must increase and the $[CH_3COOH]$ must decrease.

**Optimization of Calcium Acetate Yield using HTC shells**

A custom RSM (Response Surface Methodology) optimal design was used to optimize the yield in the fewest runs and α values of time and [$CH_3COOH$] were chosen to be round figures and allow easy performance of experiments. The factors and levels for the custom RSM design are shown in

**Table 2**. The molar [$CH_3COOH$] for this design are 0.18, 0.53, 0.88, 1.2, and 1.6 mol/L, respectively. The results of this model as well as the analysis of variance and plots of the residuals for this model are found in Supplementary Material (Tables S3-S4, Figure S4-S6).

**Table 2** Custom RSM design factors and levels for the optimization of yield of calcium acetate using HTC shells.

| Name | Factor | -α | -1 | 0 | +1 | +α |
|---|---|---|---|---|---|---|
| A | % $CH_3COOH$ | 1 | 3 | 5 | 7 | 9 |
| B | Time (h) | 16 | 20 | 24 | 28 | 32 |

The empirical model for the optimization of the response (yield) in terms of the factors studied (time, and [$CH_3COOH$]) using HTC shells is plotted in a three-dimensional diagram, **Figure 4**. This shows the model of $Ca(CH_3COO)_2$ yield based on time and [$CH_3COOH$], and shows that the $Ca(CH_3COO)_2$ yield increases as time and [$CH_3COOH$] increase. This contrasts with the exploratory experiments where the yield increases as the [$CH_3COOH$] decreased. However, at lower [$CH_3COOH$] the yields are still quite good and higher than those observed in the exploratory CCD experiments because of increased time. The highest $Ca(CH_3COO)_2$ yield achieved using HTC shells was very good, 93% after 32 h using 9% $CH_3COOH$. 90% yield was obtained after 24 h using 9% $CH_3COOH$. Therefore, a maximum $Ca(CH_3COO)_2$ yield is achieved at times greater

than 24 h using 9% $CH_3COOH$ and is a 16% yield improvement upon results from the exploratory model. $Ca(CH_3COO)_2$ yields may still have increased beyond 32 h, however, they were not explored because a >90% yield was deemed satisfactory. A yield of 90% was also found after 32 h using 1% $CH_3COOH$. While it is good that such a dilute solution can make $Ca(CH_3COO)_2$, a significant amount of additional water is required at this concentration of $CH_3COOH$ in comparison to 9% $CH_3COOH$ and this could be thought of as less environmentally friendly because clean water is a valuable resource.

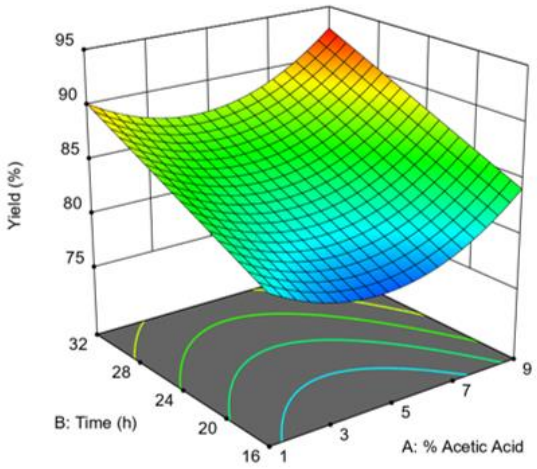


**Figure 4** The response surface plot of the optimization of $Ca(CH_3COO)_2$ yield based on concentration of acetic acid and time using heated mussel shells (HTC).

During experimentation for the synthesis of $Ca(CH_3COO)_2$, anytime a concentration of 5% $CH_3COOH$ was required, Heinz brand vinegar, i.e. food-grade vinegar, was used. This was trialed to demonstrate the ease of this synthesis and the relative safety associated with the starting materials. Anyone could make $Ca(CH_3COO)_2$ with vinegar and waste BM mussel shells and get a yield of 75-80% in 24 h. Whilst shipping would be more economical if glacial acetic acid was purchased because of the smaller volumes to be shipped – a full life cycle and cost analysis would need to be performed if this process was to be scaled up and performed commercially. Ideally, if

there were a source of biomass locally that could be fermented to produce $CH_3COOH$ – that would be an avenue worth pursuing. It has been shown by others that bamboo vinegar can be used to make de-icer,[19] the concentration of $CH_3COOH$ is low and this would work well to produce $Ca(CH_3COO)_2$.

**Characterization of Calcium Acetate**

In order to demonstrate that the HTC shells could produce $Ca(CH_3COO)_2$ of a similar quality to traditional mineral sources of calcium carbonate, optical calcite was also used as a starting material to make it. The $Ca(CH_3COO)_2$ products from both shell and optical calcite routes were characterized using a range of methods as different hydrates and anhydrous forms of this salt exist. Often calcium acetate is a monohydrate. Figure 6 shows the overlay of IR spectra for $Ca(CH_3COO)_2$ products made using CC, RTC, HTC, and optical calcite in the 400–1800 $cm^{-1}$ region. These spectra demonstrate that each $CaCO_3$ starting material is making the same form of $Ca(CH_3COO)_2$. Through comparison with literature values for calcium acetate monohydrate ($Ca(CH_3COO)_2 \cdot H_2O$) it is possible to confirm our product (from RTC, HTC and optical calcite) is indeed the monohydrate.[26, 27] The hemihydrate has additional absorptions at 1610 $cm^{-1}$ and 643 $cm^{-1}$, and the band at 945 $cm^{-1}$ in the monohydrate would appear at 947 $cm^{-1}$ in the hemihydrate.[26, 27] This is observed for $Ca(CH_3COO)_2$ made from CC shells (red) in Figure 5. It is likely that CaO starting material makes the hemihydrate rather than the monohydrate. This is further evidenced by the differences in bands in the 2500–4000 $cm^{-1}$ region where differences in water are seen, Figure 6. Several samples were tested to confirm this result. Additionally, the CC starting material may still contain some $CaCO_3$ (i.e. incomplete calcination) and a mixture of the mono- and hemihydrate may be present. This was an additional reason why the CC shells were not pursued further as a

starting material as they made a different product than what is desired and for all other analyses, $Ca(CH_3COO)_2$ made from CC shells is excluded.

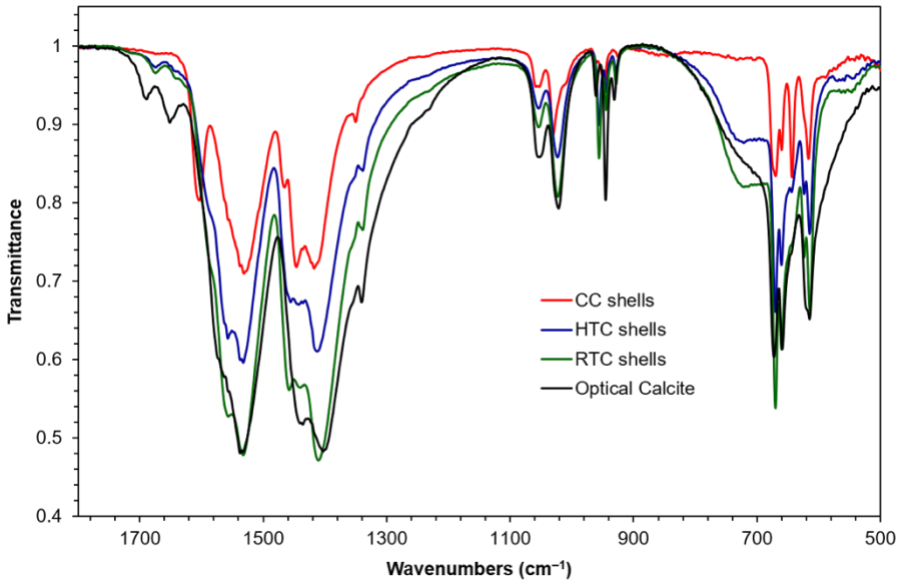


**Figure 5** Infrared spectra for $Ca(CH_3COO)_2$ products made using CC, RTC, HTC and optical calcite in the 400–1800 $cm^{-1}$ region.

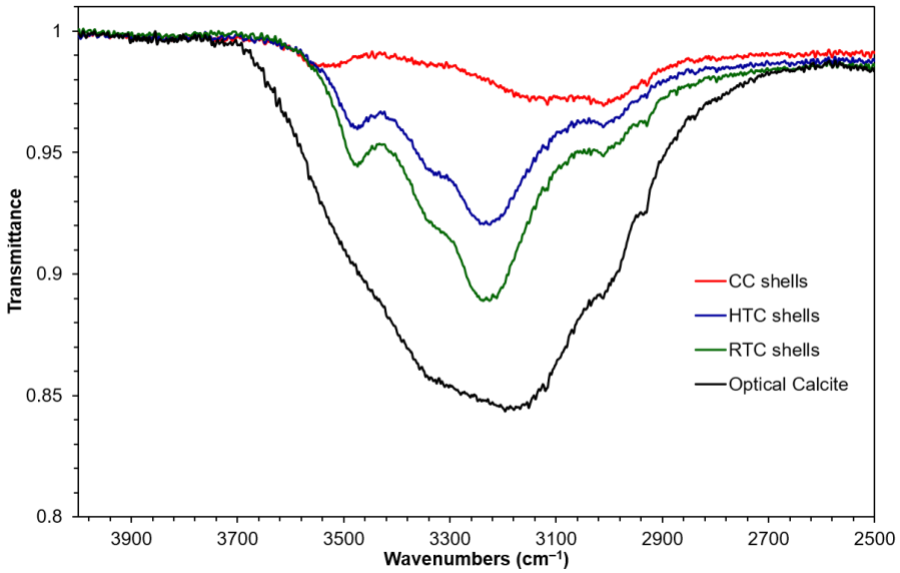


**Figure 6** Infrared spectra for $Ca(CH_3COO)_2$ products made using CC, RTC, HTC, and optical calcite showing the 2500–4000 $cm^{-1}$ region where there are clear differences in bands from water.

Thermogravimetric analysis (TGA), Figures 7 and 8, of $Ca(CH_3COO)_2$ from HTC and optical calcite confirmed what was observed by IR spectroscopy. The mass losses for $Ca(CH_3COO)_2$ from optical calcite and HTC starting materials were consistent with calcium acetate monohydrate, $Ca(CH_3COO)_2 \cdot H_2O$, from herein referred to as monohydrate.[26, 28, 29] Water loss occurs in two steps of unequal masses, the first ¾ $H_2O$ and the second ¼ $H_2O$ from 85-215 °C. The mass losses totalled 10.2 and 10.3% for the monohydrate prepared from optical calcite and HTC, respectively, which is in good agreement with the theoretical mass loss of 10.2%. After a mass loss of acetone, $CH_3COCH_3$, produced via decomposition of the anion at 550 °C, the total mass losses for the monohydrate prepared from optical calcite and HTC were 42.8 and 41.5 %, respectively. The $Ca(CH_3COO)_2 \cdot H_2O$ from optical calcite matches the theoretical value of 43.2 very well, whereas the mass loss due to acetone for HTC is slightly lower than expected. In Figure 8, which shows to the thermal analysis of $Ca(CH_3COO)_2 \cdot H_2O$ from HTC, there is an additional mass loss of 0.74% that is not present in the monohydrate from optical calcite. This mass loss is also present in the thermal analysis of mussel shells.[34,35] This mass loss is due to contamination of the monohydrate with organic matrix from the shell and is likely the reason why the mass losses of the monohydrate from HTC do not match the theoretical values perfectly. This is a limitation to the use of mollusc shells as a starting material to make chemicals where purity is a concern (i.e. pharmaceuticals).

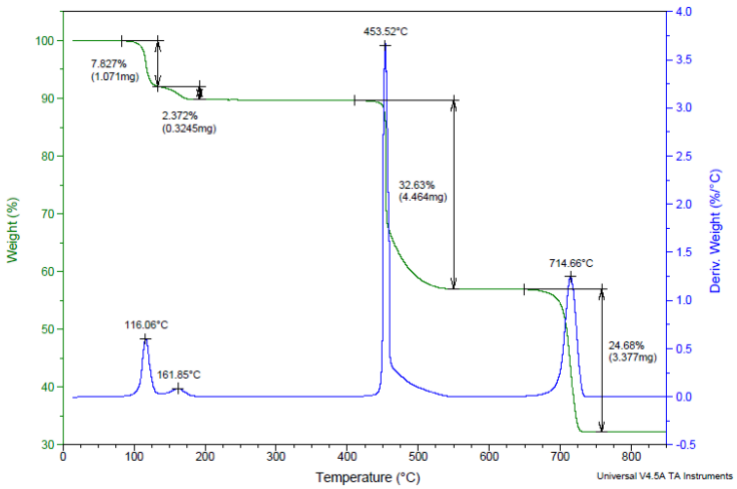


**Figure 7** Thermogravimetric analysis for calcium acetate monohydrate ($Ca(CH_3COO)_2{\cdot}H_2O$) made using optical calcite.

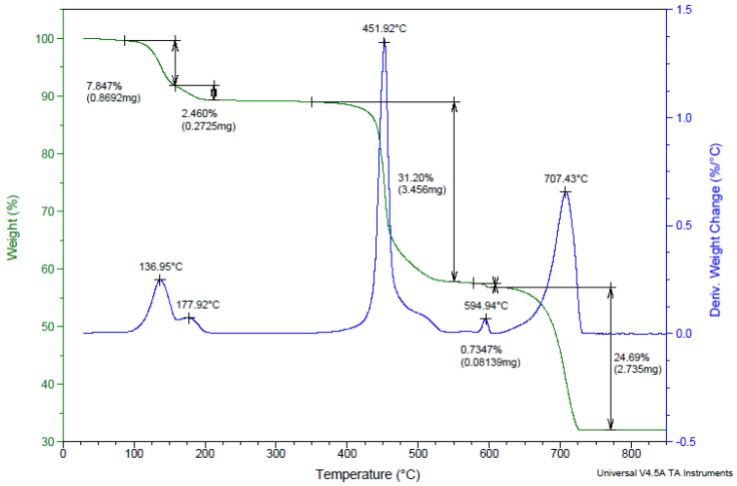


**Figure 8** Thermogravimetric analysis for calcium acetate monohydrate ($Ca(CH_3COO)_2{\cdot}H_2O$) made using HTC shells.

The morphology of $Ca(CH_3COO)_2{\cdot}H_2O$ is very different from NaCl which leads to challenges in its use as a de-icer. Images from the crystallization of $Ca(CH_3COO)_2{\cdot}H_2O$, Figure 9, show it grows in tight bundles of thin crystalline needles with air gaps, which means it has a relatively low density that makes it difficult to apply to roads especially in regions with high winds such as Newfoundland. Instead of going directly on the road, $Ca(CH_3COO)_2$ could be applied as a

brine or applied to the surface of adhesives (i.e. sand or crushed shells). Cryotech Inc., a company that sells similar de-icing and anti-ice agents, has a patented technology to make pellets with acetate de-icers to overcome the high dust challenges.[17] Scanning electron microscopy (SEM) images of a $Ca(CH_3COO)_2$ sample prepared in this study shows the tight needle organization, Figure 10, which is similar to what was observed for the calcite layer of mussel shells. The prismatic orientation of $Ca(CH_3COO)_2 \cdot H_2O$ synthesized using HTC shells is different from commercial $Ca(CH_3COO)_2 \cdot H_2O$ and $Ca(CH_3COO)_2 \cdot H_2O$ prepared from butter clam shells.[24] It is well known that additives including macromolecules and amino acids can change the crystal shape of calcite, and this might also apply to other calcium-containing salts.[30-32]

**Figure 9** Photographs of $Ca(CH_3COO)_2 \cdot H_2O$ made from shells that show crystal growth upon evaporation of water.

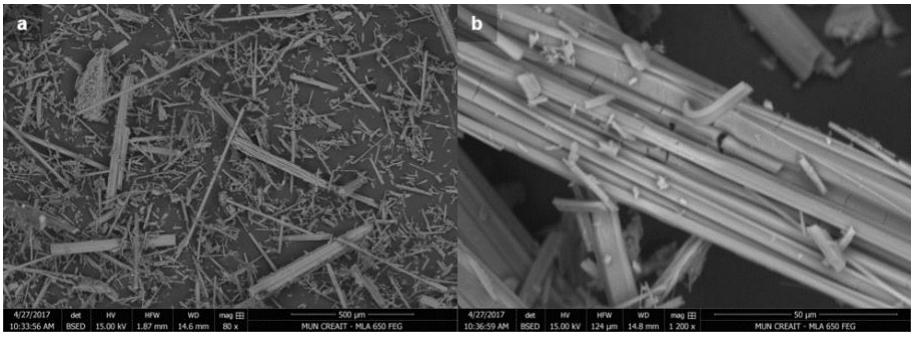


**Figure 10** Scanning electron micrographs (back-scattered) of calcium acetate monohydrate made from HTC shells at various magnifications.

The likely presence of organic matrix in the product via TGA data and differences in crystal shape between $Ca(CH_3COO)_2{\cdot}H_2O$ from HTC compared to commercial $Ca(CH_3COO)_2{\cdot}H_2O$ prompted X-ray diffraction analysis of $Ca(CH_3COO)_2{\cdot}H_2O$ from optical calcite compared with $Ca(CH_3COO)_2{\cdot}H_2O$ from HTC shells. Diffractograms are shown in Figure 11 for the two $Ca(CH_3COO)_2{\cdot}H_2O$ products along with a simulated powder spectrum from cif data for $Ca(CH_3COO)_2{\cdot}H_2O$,[33] zoomed in regions of these diffractogram are shown in Supplementary Material (Figures S7-S9). The peaks for the reflections in $Ca(CH_3COO)_2{\cdot}H_2O$ made from optical calcite and HTC match with the simulated powder diffractogram from cif data of $Ca(CH_3COO)_2{\cdot}H_2O$[33] and agree with observations from IR and TGA. The products are calcium acetate monohydrate, despite differences in relative intensities of the reflections and slight shifts in peak positions. This could have been corrected (i.e indexed or fitted) however it was not deemed necessary based on the supporting chemical characterization. The shift is most likely due to a raise or dip in the sample, from sample prep. Going from optical calcite to HTC, the 0 –1 0 intensity increases, and the 0 1 –2 intensity decreases. This suggests the $Ca(CH_3COO)_2{\cdot}H_2O$ made from HTC crystallizes differently (i.e. preferentially from a different face).

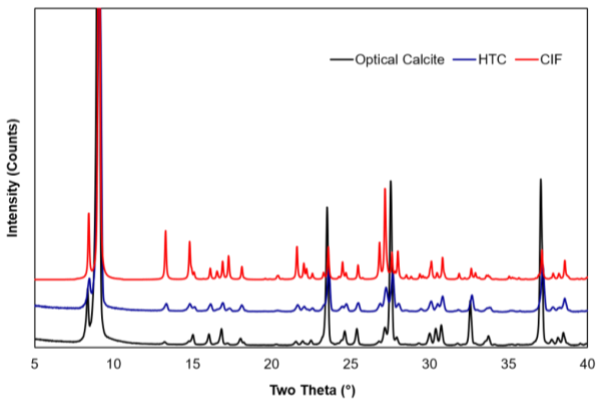


**Figure 11** Powder X-ray diffractograms of $Ca(CH_3COO)_2{\cdot}H_2O$ made from optical calcite and HTC shells plotted with the simulated diffractogram from the crystallographic information file (CIF). CCDC 1122640.

## De-icing Experiments

De-icing experiments were carried out using $Ca(CH_3COO)_2{\cdot}H_2O$ made from HTC shells to assess the efficacy of $Ca(CH_3COO)_2{\cdot}H_2O$ as a de-icer. Others have already reported the successful use of $Ca(CH_3COO)_2{\cdot}H_2O$ as a de-icer.[19, 22] Because of limitations of dealing with $Ca(CH_3COO)_2{\cdot}H_2O$ in solid form (i.e. dust issues), $Ca(CH_3COO)_2$ solutions at various concentrations were prepared and application as a brine was explored. Concentrations of $CaMg_2(CH_3COO)_6$ are typically 30% (m/v)[14], therefore concentrations up to 30% of $Ca(CH_3COO)_2{\cdot}H_2O$ were trialed. Experiments were performed at a single temperature but in a similar fashion to previous researchers.[19]

**Table 3** Data for de-icing experiments performed at different concentrations of calcium acetate brine applied to ice and reported as mass losses and gains at –16°C.

| **Concentration of $Ca(CH_3COO)_2{\cdot}H_2O$** | **Percent loss or gain of water mass (%)** |
|---|---|
| Blank – Distilled water | + 14.0 ± 0.40 |
| 15% | + 0.85 ± 0.05 |
| 20% | - 1.8 ± 0.10 |
| 25% | - 4.0 ± 0.10 |
| 30% | - 5.6 ± 0.20 |

Based on de-icing experiments, calcium acetate does melt ice (
Table **3**) but the concentration used is very important. The blank experiment, where 10.0 mL of water was added to ice saw an increase of mass by 14%. A solution of 15% $Ca(CH_3COO)_2{\cdot}H_2O$ was not suitable for de-icing as the mass of water (ice) increased (0.85%) after 15 minutes (Figure S10). De-icing experiments showed that the $Ca(CH_3COO)_2{\cdot}H_2O$ produced from waste BM melted 5.6 ± 0.2 wt.% of ice in 15 minutes at concentrations of 30% (m/v) at –16 °C.

These concentrations can be compared with previously reported studies. For example, $CaMg_2(CH_3COO)_6$ is commonly administered at 25%, $K(CH_3COO)$ is 50%, $MgCl_2$ and $CaCl_2$ are 30%, and NaCl, if used as a brine is 23%.[14] In order to standardize our method, we performed de-icing experiments using CaCl2 and NaCl brines across the same time frames, concentrations and using identical freezers/equipment (Figures S11 and S12). These showed that the $CaCl_2$ melted 11.4 ± 0.95 wt.% and NaCl melted 12.6 ± 0.42 wt.% of ice in 15 minutes at concentrations of 30% (m/v) at –16 °C. These show that under our conditions $Ca(CH_3COO)_2$ is not as efficient as traditional chloride de-icers. In earlier studies, Jiang *et al.* performed de-icing experiments at 0 °C using solid $Ca(CH_3COO)_2$ prepared from distilled bamboo vinegar (0.478 mol/L) and $Ca(OH)_2$.[19] They reported that 28% of ice was melted after 1 h using 2 g of $Ca(CH_3COO)_2$ on 100 g of ice. The patent from South Korea reports 25-30% (m/v) of $Ca(CH_3COO)_2$ is used for de-icing but does not report detailed results.[22]

## Conclusions

Three starting materials sourced from waste mussel shells were screened for the synthesis of calcium acetate using acetic acid. The three materials were shells without heat treatment, shells heated to 220 °C for 48 h and shells calcined to yield CaO. An exploratory CCD compared the yield of $Ca(CH_3COO)_2{\cdot}H_2O$ with respect to shell type, concentration of $CH_3COOH$, and time. Calcined shells resulted in poor yields, regardless of time and $CH_3COOH$ concentrations and the heat-treated shells afforded the best yields. Characterization data confirmed that the product of these reactions was a monohydrate. The yield of $Ca(CH_3COO)_2{\cdot}H_2O$ was further optimized using using a custom optimal design with longer reaction times and low $CH_3COOH$ concentrations. A maximum yield of 93% was reached after 32 h using 9% $CH_3COOH$. Other concentrations of

$CH_3COOH$ were still very successful and using food-grade white vinegar, an 85% yield of $Ca(CH_3COO)_2{\cdot}H_2O$ was obtained after 24 h. The product monohydrate was characterized by IR spectroscopy, TGA and powder XRD. The $Ca(CH_3COO)_2{\cdot}H_2O$ produced from BM shells HTC and RTC were the same as using pure $CaCO_3$ in the form of optical calcite. The morphology of $Ca(CH_3COO)_2{\cdot}H_2O$ was prismatic like the outer calcite layer of mussel shells.[35] Powder XRD data suggest that the organic matrix from the shell is directing crystal growth because the reflection intensities of $Ca(CH_3COO)_2{\cdot}H_2O$ produced using HTC differ from those for $Ca(CH_3COO)_2{\cdot}H_2O$ prepared from optical calcite. De-icing experiments showed that the $Ca(CH_3COO)_2{\cdot}H_2O$ produced from waste BM melted 5.6 ± 0.2 wt.% of ice in 15 minutes at concentrations of 30% (m/v) at –16 °C. This is very promising for progress towards a sustainable, non-corrosive and degradable de-icer; however, sustainability can be further improved is a renewable source of $CH_3COOH$ was identified and used. Unfortunately, this de-icer is much less efficient than chloride-containing brines.

## Experimental

### General Considerations

Glacial acetic acid (99.9%) was purchased from Fisher Scientific and used without purification. Optical calcite was purchased from a mineral supply store in Colorado and is from Mexico originally. Blue mussels and Heinz brand vinegar were purchased at Sobeys supermarket, St. John's. Shells were cleaned, removing any organic material, using industrially available food grade protease enzymes as previously described.[34] Cleaned mussel shells were dried at 220 °C for 48 h (HTC) or calcined at 750 °C for 4 h in a tube furnace under air (CC). A SPEX mixer mill equipped with a 65 mL stainless steel vial with two quarter inch stainless steel balls was used to grind shells

for 12 min in initial experiments. Upon discovery of iron contamination in ground shells, experiments were performed using shells that were crushed to >2 cm size flakes manually.

Infrared (IR) spectroscopy was performed using a Bruker Alpha FTIR spectrometer fitted with a single bounce diamond ATR accessory at a resolution of 2 $cm^{-1}$. All measurements were conducted in triplicate, averaged and plotted in Excel. Thermogravimetric analysis (TGA) was carried out using a TA Instruments Q500 under a $N_2$ atmosphere (50 mL $min^{-1}$) from 25-850 °C. Scanning electron microscopy (SEM) images were obtained using a FEI MLA 650 FEG under high vacuum ($10^{-6}$ torr). The voltage of 15 kV and current of 10 mA at a working distance of 14.9 mm produced a 5.8 spot. An SDD was used for BSED. Powder X-ray diffraction (XRD) was performed using a Rigaku MiniFlex XRD equipped with Cu Kα radiation (λ=1.5406 Å). The 2θ region was scanned from 0-50° with a step size of 0.02°.

**Synthesis of Calcium Acetate**

Approximately 3 g of shells were weighed directly into an Erlenmeyer flask. The exact mass of shells was noted and the required volume of $CH_3COOH$ was added. The size of the flask varied as the concentration and volume of $CH_3COOH$ used was varied. For example, if 38 mL of 9% $CH_3COOH$ was required, a 125 mL Erlenmeyer was used but if 341 mL of 1% $CH_3COOH$ was required a 500 mL Erlenmeyer was used. All reactions were stirred magnetically at room temperature. Once the reaction was complete, the pH was tested with full range pH paper. If the pH paper did not indicate a neutral pH, small quantities of NaOH (3 mol/L) were added until the pH reached 7. The reaction mixture was gravity filtered, and the calcium acetate solution was collected in a beaker. The solution was heated on a hot plate until most of the water evaporated. This was to speed up the crystallization of calcium acetate because it is very soluble in water. Once crystallization was complete, samples were left at room temperature for three days to achieve

constant mass before being weighed to calculate yields. This was preferred over drying in an oven so that the products remained monohydrates. Any unreacted shells, as the residue from the filtration step, were kept to prepare high surface area calcite (soft calcite).

**De-icing Experimental Procedure**

Experiments were performed at a single temperature but in a similar fashion to previous researchers.[19] Ice was prepared by placing 50.0 mL of water in a 250.0 mL Erlenmeyer flask and placing the flask in the freezer at –16 °C for 5 h. $Ca(CH_3COO)_2$ solutions in concentrations of 15, 20, 25, and 30% (m/v) were prepared to a final volume of 10.0 mL. The $Ca(CH_3COO)_2$ solutions were chilled at 5 °C for 1 h prior to adding the brine to the ice. The brine was added to the ice and remained in freezer for 15 min after which any liquid was decanted (using a Pasteur pipette), the mass of ice left over was recorded, and percent of ice removed was calculated. Experiments were also performed using the same concentrations of calcium chloride and sodium chloride. All experiments were performed in triplicate (Figures S10-12).

**Supplementary Material**

Yields, data, plots and analysis from CCC and custom design experiments. Expanded regions for powder X-ray diffractograms. % ice melted against concentration of brine % m/v graphs.

**Acknowledgements**

Memorial University and NSERC of Canada are thanked for operating funds and scholarship funds. Dr. Liqin Chen is also acknowledged for scholarship funding. CFI and the Government of Newfoundland and Labrador are thanked for infrastructure grants. We thank Memorial University's CREAIT Network for access to instruments and their management.

## References


1. Y. Hou, A. Shavandi, A. Carne, A. A. Bekhit, T. B. Ng, R. C. F. Cheung and A. E.-d. A. Bekhit, *Crit. Rev. Environ. Sci. Technol.*, 2016, **46**, 1047-1116.
2. J. N. Murphy and F. M. Kerton, in *Fuels, Chemicals and Materials form the Oceans and Aquatic Sources* eds. F. M. Kerton and N. Yan, Wiley, 2017, ch. Characterization and utilization of waste streams from mollusc aquaculture and fishing industries, pp. 189-225.
3. J. P. Morris, T. Backeljau and G. Chapelle, *Rev. Aquacult.*, 2018, **11**, 42-57.
4. N. Seco-Reigosa, S. Pena-Rodriguez, J. C. Novoa-Munoz, M. Arias-Estevez, M. J. Fernandez-Sanjurjo, E. Alvarez-Rodriguez and A. Nunez-Delgado, *Environ. Sci. Pollut. Res.*, 2013, **20**, 2670-2678.
5. A. M. Ramirez-Perez, M. Paradelo, J. C. Novoa-Munoz, M. Arias-Estevez, M. J. Fernandez-Sanjurjo, E. Alvarez-Rodriguez and A. Nunez-Delgado, *J. Hazard. Mater.*, 2013, **248-249**, 122-130.
6. M. C. Barros, P. M. Bello, M. Bao and J. J. Torrado, *J. Clean Prod.*, 2009, **17**, 400-407.
7. M. L. Mai, M. Emmett, M. S. Sheikh, C. A. Santa Ana, L. Schiller and J. S. Fordtran, *Kidney Int.*, 1989, **36**, 690-695.
8. M. Wei, A. J. Ruys, B. K. Milthorpe and C. C. Sorrell, *J. Mater. Sci.: Mater. Med.*, 2005, **16**, 319-324.
9. Health Canada, https://www.canada.ca/en/health-canada/services/food-nutrition/food-safety/food-additives/lists-permitted/10-adjusting-agents.html, (accessed December 27, 2024).
10. K. Wang, D. E. Nelsen and W. A. Nixon, *Cem. Concr. Compos.*, 2006, **28**, 173-188.

11. *Environment Canada, 2001. Canadian Environmental Protection Act, 1999, Priority Substances List Assessment Report – Road Salt*, Environment Canada, Hull, Quebec.

12. M. S. Perchanok, D. G. Manning and J. J. Armstrong, *Highway deicers: Standards, practice and research in the Province of Ontario*, R. a. D. Branch, Downsview, Ontario, 1991.

13. S. S. Kaushal, *Environ. Sci. Technol.*, 2016, **50**, 2765-2766.

14. M. Fischel, *Evaluation of Selected Deicers Based on a Review of the Literature*, Report No. CDOT-DTD-R-2001-15, Denver, CO, 2001.

15. D. M. Ramakrishna and T. Viraraghavan, *Water, Air, Soil Pollut.*, 2005, **166**, 49-63.

16. M. C. Santagata and M. Collepardi, *Cem. Concr. Res.*, 2000, **30**, 1389-1394.

17. Cryrotech, http://www.cryotech.com/commercial, (accessed December 27, 2024).

18. W. Fu and A. P. Mathews, *Enzyme Microb. Tech.*, 2005, **36**, 953-959.

19. X. Jiang, G. Li and Z. Wu, *World Academy of Science, Engineering and Technology International Journal of Chemical and Molecular Engineering*, 2010, **4**, 304-309.

20. B. Yun Yang and R. Montgomery, *Bioresource Technol.*, 2003, **90**, 265-273.

21. J. Liu, Y. Zhang, Y. Liu, H. Liu and D. Xing, *Guangdong Huagong*, 2012, **39**, 24-26.

22. 'Preparation method of snow removing materials by using oyster shell', *South Korea Pat.*, KR101328694B1, application filed 2011, application granted 2013.

23. Z. Fan, X. Yang, J.-q. Guan, J. Zhang, L. Qiao and X.-y. Chang, *Shipin Gongye Keji*, 2015, **36**, 254-258.

24. H. J. Lee, N. Y. Jung, S. H. Park, S. M. Song, S. I. Kang, J.-S. Kim and M. S. Heu, *J. Korean Soc. Food Sci. Nutr.*, 2015, **44**, 888-895.

25. T. Di Nardo and A. Moores, *Beilstein J. Org. Chem.*, 2019, **15**, 1217-1225.

26. N. H. Tennent and T. Baird, *Stud. Conserv.*, 1985, **30**, 73-85.

27. A. W. Musumeci, R. L. Frost and E. R. Waclawik, *Spectrochim. Acta A*, 2007, **67**, 649-661.

28. D. Asmi and I. M. Low, *Ceram. Int.*, 2008, **34**, 311-316.

29. A. T. Pemberton, D. B. Magers and D. A. King, *J. Chem. Ed.*, 2019, **96**, 132-136.

30. Y.-Y. Kim, J. D. Carloni, B. Demarchi, D. Sparks, D. G. Reid, Miki E. Kunitake, C. C. Tang, M. J. Duer, C. L. Freeman, B. Pokroy, K. Penkman, J. H. Harding, L. A. Estroff, S. P. Baker and F. C. Meldrum, *Nat. Mater.*, 2016, **15**, 903-910.

31. L.-B. Mao, H.-L. Gao, H.-B. Yao, L. Liu, H. Cölfen, G. Liu, S.-M. Chen, S.-K. Li, Y.-X. Yan, Y.-Y. Liu and S.-H. Yu, *Science*, 2016, **354**, 107-110.

32. H.-L. Gao, S.-M. Chen, L.-B. Mao, Z.-Q. Song, H.-B. Yao, H. Cölfen, X.-S. Luo, F. Zhang, Z. Pan, Y.-F. Meng, Y. Ni and S.-H. Yu, *Nat. Commun.*, 2017, **8**, 287.

33. E. A. Klop, A. Schouten, P. van der Sluis and A. L. Spek, *Acta Crystallogr. C*, 1984, **40**, 51-53.

34. J. N. Murphy, K. Hawboldt and F. M. Kerton, *Green Chem.*, 2018, **20**, 2913-2920.

35. J. N. Murphy, C. M. Schneider, L. K. Mailänder, Q. Lepillet, K. Hawboldt and F. M. Kerton, *Green Chem*., 2019, **21**, 3920-3929

## Graphical Abstract Use Only